Journal of Mines, Metals and Fuels, *71(12A): 297-304; 2023. DOI: 10.18311/jmmf/2023/44006*

Print ISSN : 0022-2755

Journal of Mines, Metals and Fuels

Contents available at: *www.informaticsjournals.com/index.php/jmmf*

Effect of Triggering Mechanism and Variable Strain Rates on Energy Absorption of Glass Fiber Reinforced Polymer Tubes Under Quasi Static Compression

K. Y. Chethana[1], M. R. Srinivasa[2], Y. S. Rammohan[1], M. G. Patil[3], M. Ravikumar[3], Raghu Yogaraju[3] and A. R. Aparna[1]

[1]*Department of Aerospace Engineering, B. M. S. College of Engineering, Bengaluru – 560019, Karnataka, India; chethanaky.aer@bmsce.ac.in*

[2]*Department of Mechanical Engineering, PES College of Engineering, Mandya – 571401, Karnataka, India*

[3]*Department of Mechanical Engineering, B. M. S. College of Engineering, Bengaluru – 560019, Karnataka, India*

Abstract

Fiber-reinforced polymer matrix (FRP) composites have evolved as a prominent class of structural materials for usage as thin-walled impact-absorbing structural members in the case of industries such as aerospace, marine, and automotive. The experimental studies began with the literature survey, identification of the best method of the fabrication process, and new method of fabrication of specimen to trigger the steady crushing process. Which were then subjected to the axial compression test. The tubular Glass Fiber Reinforced Polymer (GFRP) composite tubes were made utilizing woven glass fabric plies in a manual wrap-up approach. The axial compression test was used to determine the absorbed energy of each GFRP composite at a variable strain rate. Finally, a relative assessment of the energy absorption capabilities of specimens was established in order to study deformation mechanism and their energy absorption capability.

Keywords: *Energy Absorption, FRP, Impact Energy, Strain Rates*

1.0 Introduction

The attention to thin-walled energy retaining tubes for crashworthiness applications has been becoming greater over time because of the increment of the security cognizant climate in the significant transportation industry, for example, auto and aviation[1]. The crashworthy tube structures in energy assimilation are manufactured from a different solid material, for example, metallic, engineered fiber, and a combination of metallic and fiber with different sorts of polymer. Accordingly, the utilization of thin wall crashworthy structure in automotive, elite motorsport[2] where the front rails in vehicles and the pound safeguard of trains and vehicles[3,4] which has been known as front-facing rail cylinder or front-facing longitudinal cylinder[4], where it will act as a sacrificial member by absorbing impact load. There are a large variety of impact energy devices ranging from sand drags and shredded paper to structural elements (such as beam, plate, and shell-type devices) custom-made honeycombs. A fracture occurs when the capacity for plastic deformation ceases[5,6]. Fracture without plastic deformation requires little energy only which is needed to create new surfaces. Hence a very large number of fractures that lead to fragmentation and pulverization in brittle materials are essential to dissipate any appreciable

**Author for correspondence*

amount of energy. Fiber-reinforced plastic elements are coming increasingly into practical use. The analyze and design such energy absorbers, it is essential to understand the materials behavior, under high strain rate and low strain rate conditions under different modes of loading. A few studies have been conducted to examine how strain rate affects composite materials' energy-absorbing limit, Despite the fact that Glass fiber tubes showed the lowest mechanical characteristics and absorption of specific energy under compression load[8]. It can be examined at a variable strain rate. Marc Mayer *et al.*[7,9] has authored the book and an article. Regarding mechanics and materials methods, this offers a thorough and introductory discussion of the mechanical behaviour of the materials. Additionally, it highlights fracture criteria and plastic deformation.

2.0 Materials and Methods

Polymer composite tubes were made from an E-glass fiber mat of 200 gsm, 300gsm, 450gsm and Matrix as polyester resin with hardener Methyl Ethyl Ketone Peroxide.

An initial chamfer of 45^0 will give to GFRP tubes to trigger the progressive damage; the composition of self-triggered tube is 200 gsm, 300 gsm and 450 gsm layers starting with 200 gsm at the inside layer of the tube. The 200 gsm layer at the inner end has lowest SEA and 450 gsm layer has the maximum SEA. Therefore, there is no requirement of giving 45^0 chamfer to initiate progressive deformation. The composition of graded layers itself helps in progressive deformation.

3.0 Scope

The investigation is aimed at examining the GFRP tubes crushed under different low strain rates of $1.1x10^{-3}$/s, $2.2x10^{-3}$/s, and $3.3x10^{-3}$/s and to quantify the energy ingestion under the above conditions.

4.0 Objectives

In order to conduct an experimental study about the crushing behaviour of Non triggered and self-triggered GFRP tubes subjected to low strain rates of $1.1x10^{-3}$/s, $2.2x10^{-3}$/s, and $3.3x10^{-3}$/s. To quantify the energy absorption of GFRP tubes under the above strain rates conditions.

5.0 Experimental Investigations

The GFRP tubes were subjected to a series of unidirectional crushing tests, yielding the experimental findings. The current investigation focuses on how low strain rates and triggering mechanisms affect tubes' deformation behaviour and GFRP tubes' ability to absorb energy.

The tubes were undergone different machining processes like edge filing and cutting to acquire desired slenderness ratio (L/d) of less than 3 to avoid Euler's buckling and They underwent quasi-static compression testing.

Initial adjustment for the test has made by the bottom and top flat pressure plates were fixed to the upper stationary head and lower table respectively. The tube specimen was placed on the bottom plate in order to grip it. Then zero was adjusted by lifting the lower table.

The initial length, diameter and weight of the specimen were measured as 100 mm length, 50 mm inside diameter, 52.15 mm outside diameter and 98.9 to 100 grams of weight then the tube specimen was placed on the bottom platform of the compression testing machine and make sure zero value pointer reading then the load was applied in terms of strain rate at the rate of $1.11x10^{-3}$/s for the first set of tubes or first case, $2.22x10^{-3}$/s and $3.33x10^{-3}$/s for 2^{nd} and 3^{rd} set of tubes and the corresponding load Vs displacement data recorded. Application of load on the specimen conducted till tube was completely crushed. Results, graphs and necessary data were recorded in the computer control unit.

6.0 Equipment and Testing Methods

Uni-directional axial quasi-static compression tests were carried out on UTES -40 an electronic universal testing machine of maximum capacity of 400 kN. Experimental methods are followed by the author[4]. The tubes were tested under uniaxial compressive load and in a 400kN electronic version UTM, the crushing behavior was observed; the load-displacement curves were plotted

and the energy-absorbing characteristics like initial load, energy absorbed during the plastic deformation were recorded.

7.0 Results

A progression of tests was attempted to describe the ability to absorb energy by the GFRP composite cylinders at varied strain rates, to carry out an experimental investigation on the crushing behavior of GFRP tubes subjected to low strain rates of $1.11x10^{-3}$/s, $2.22x10^{-3}$/s and $3.33x10^{-3}$/s. To calculate the amount of energy absorbed by GFRP tubes under the above strain rates conditions.

8.0 Discussion on Results

Uniaxial compression tests were conducted under different strain rates and the load-displacement curves

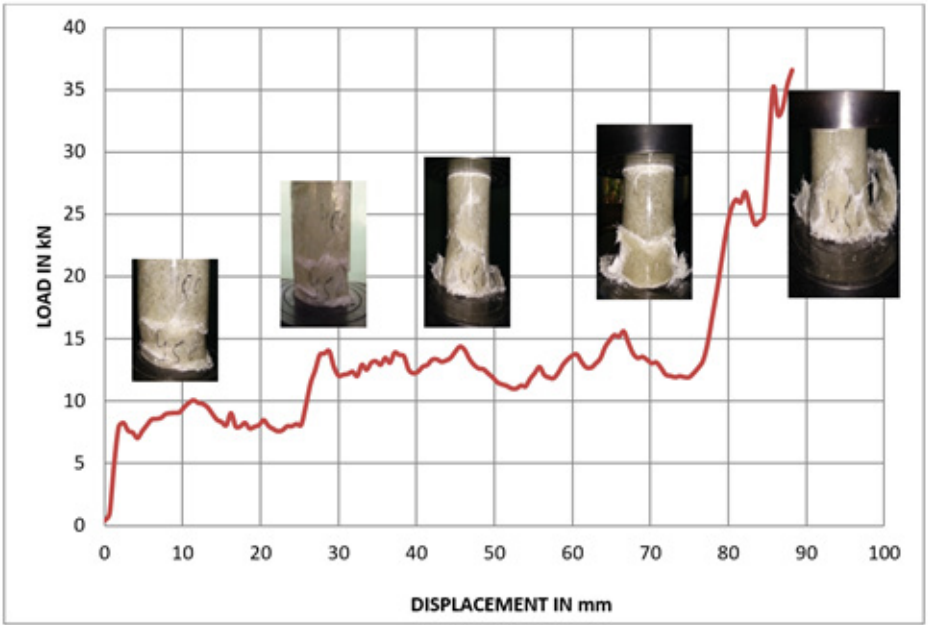

Figure 1. Load-displacement curves for 200gsm tube at strain rate $2.22x10^{-3}$/s

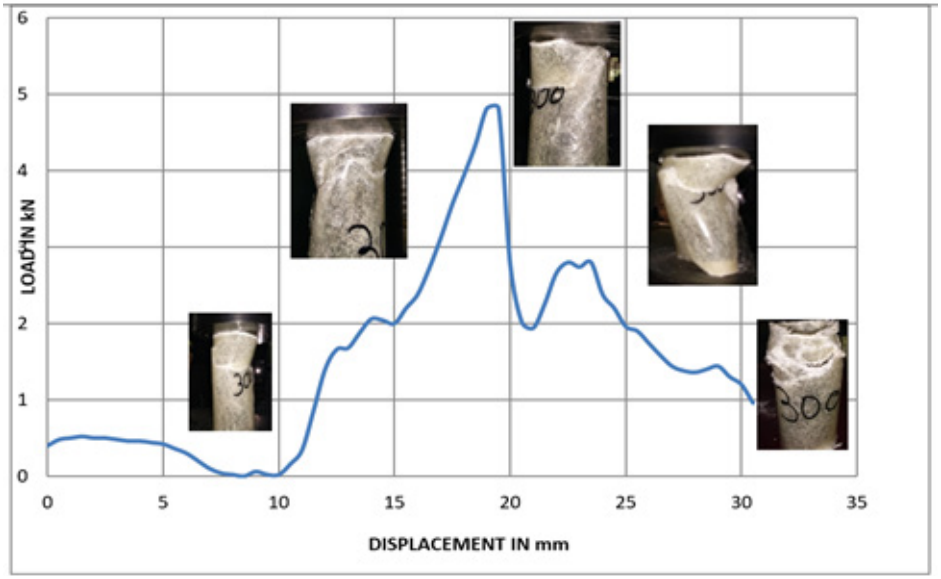

Figure 2. Load-displacement curves for 300gsm tube at strain rate $2.22x10^{-3}$/s.

were plotted for each of the test materials. From these curves, the energy-absorbing capacities were determined by tracing the area below the average load line. The average energy absorbing capacity of the GFRP tubes when compressed under a strain rate of $1.11x10^{-3}$/s, $2.22x10^{-3}$/s and $3.33x10^{-3}$/s are found to be in the order of increasing trend.

From the area under the graph shown below in the Figures 1, 2, 3 and 4, we have:

Specific energy absorption is given by:

Let the Energy absorbed = 1.429 kJ, mass of the tube = 98.9 grams then the .

NST2-Non self triggered tube of 200 gsm, NST3-Non self triggered tube of 300 gsm, NST4-Non self triggered tube of 450 gsm and ST –self triggered tube fabricated by 200 gsm, 300 gsm and 450 gsm density mats.

A typical Load –Displacement curve of an empty GFRP tube is as shown in Figure 1. along with snapshots

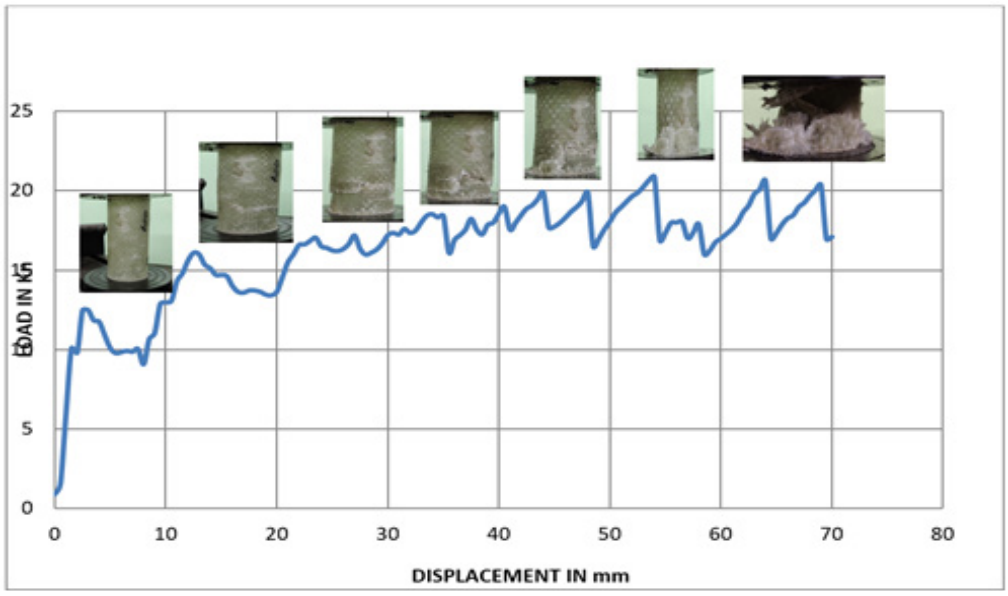

Figure 3. Load-displacement curves for 450gsm tube at strain rate $2.22x10^{-3}$/s.

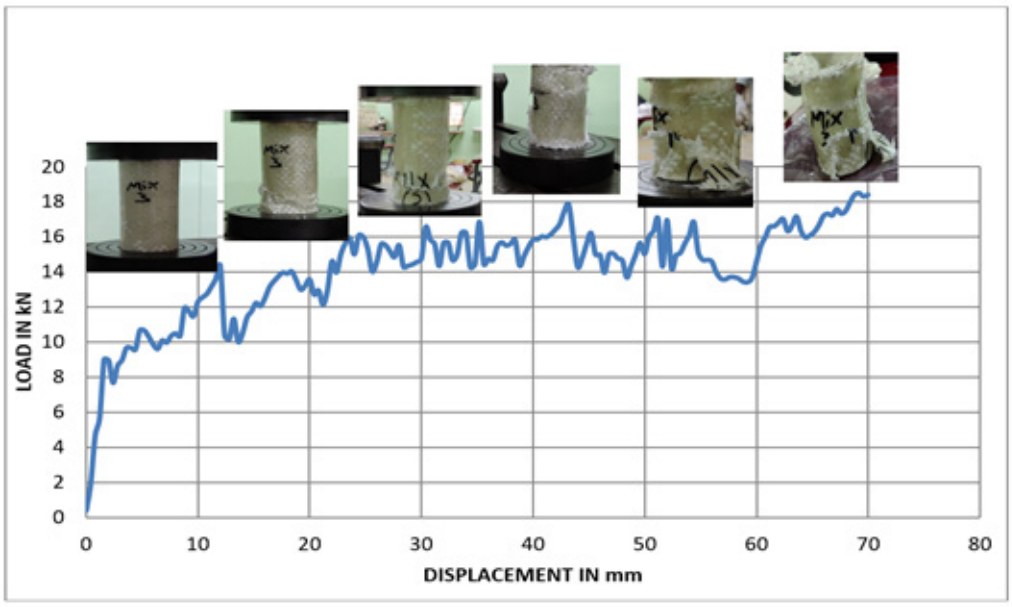

Figure 4. Load-displacement curves for self-trigger tube at strain rate $2.22x10^{-3}$/s.

of the specimen at specified stages of compression. It is observed that the load increases with displacement from the beginning of loading to the first instance of plastic buckling and then decreases abruptly followed by fluctuation about a mean as the deformation continued. Figure 1 shows the circumferential cracks formation and mechanism of deformation in the crushing tube. The respective images depicting the deformation mechanics, also the curve show the initial peak load and progressive petting zone. Figure 2 shows the load versus displacement curve when the GFRP tube is crushed under uni-directional axial compressive loading at a strain rate of $1.1x10^{-3}$/s. the chapter presents the experimental results obtained from a series of unidirectional crushing tests

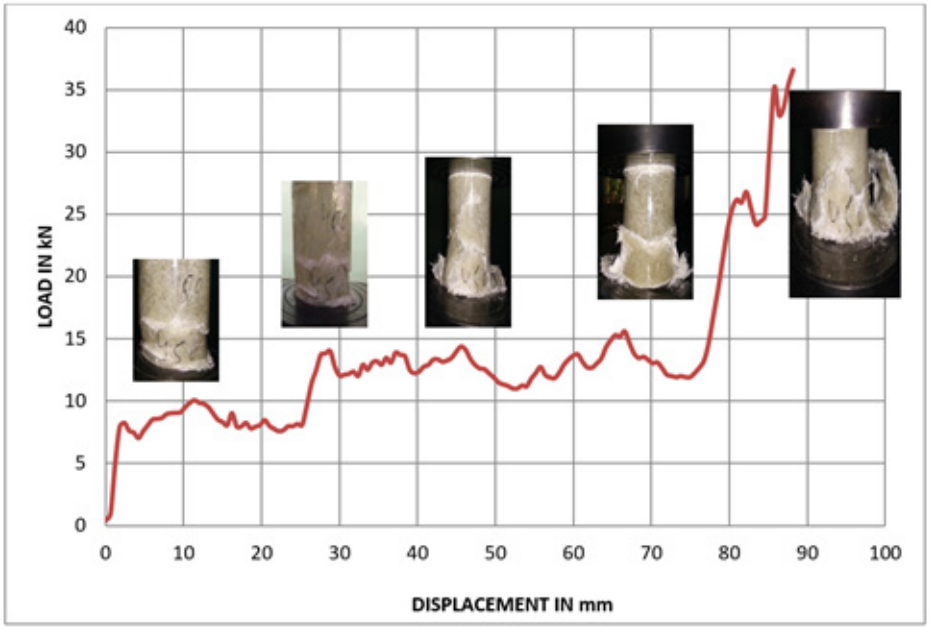

Figure 5. Load-displacement curves for 450gsm tube at strain rate $2.22x10^{-3}$/s.

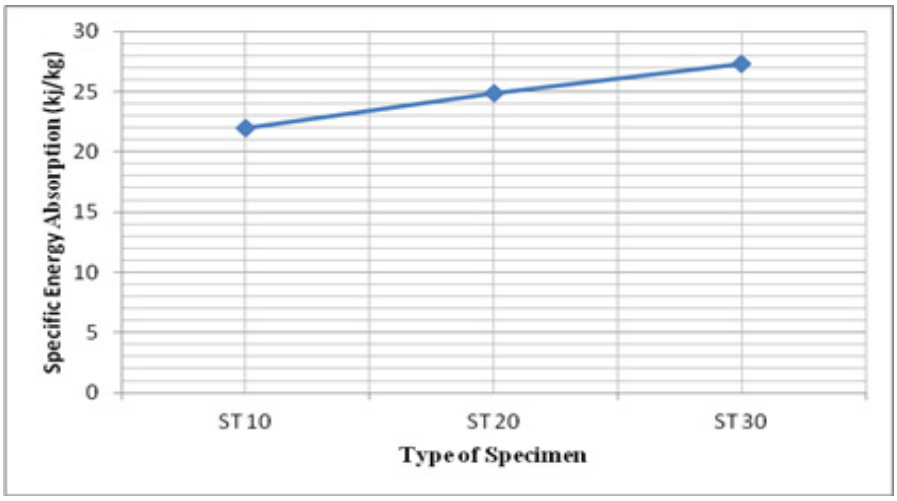

Figure 6. Quasi- static axial compression test of self-triggered tubes at a different strain rates.

ST10-Self triggered tube at $1.11x10^{-3}$ strain rate, ST20-Self triggered tube at $2.22x10^{-3}$ strain rate, and ST30-Self triggered tube at $3.33x10^{-3}$ strain rate.

Table 1. Comparative quasi- static axial compression test results of non self triggered and self triggered tubes

Deformation Rate (mm/min)	Strain Rate (/s)	Specimen Code	Energy absorbed(kJ)	Mass (gms)	Specific Energy Absorbed (kJ/kg)
20	2..22 x10^{-3}	Non self Trigger 200 gsm Tube -20-1	1.429	99	14.43
		Non self Trigger 200 gsm Tube -20-2	1.502	99.1	15.16
		Non self Trigger 200 gsm Tube -20-3	1.224	99	12.36
		Non self Trigger 200 gsm Tube -20-4	1.408	99.11	14.21
				Average	14.04
20	2..22 x10^{-3}	Non self Trigger 300 gsm Tube -20-1	2.362	99.3	23.79
		Non self Trigger 300 gsm Tube -20-2	2.426	99.3	24.43
		Non self Trigger 300 gsm Tube -20-3	2.316	99.31	23.32
		Non self Trigger 300 gsm Tube -20-4	2.107	99.31	21.22
				Average	23.18
20	2..22 x10^{-3}	Non self Trigger 450 gsm Tube -20-1	2.535	100	25.35
		Non self triggered 450 gsm Tube -20-2	2.666	99.9	26.69
		Non self triggered 450 gsm Tube -20-3	2.256	99.98	22.56
		Non self triggered 450 gsm Tube -20-4	2.414	99.98	24.14
				Average	24.69

20	2..22 x10^{-3}	Self triggered Tube -20-1	2.535	99.8	25.4
		Self triggered Tube Tube -20-2	2.666	99.5	26.79
		Self triggered Tube Tube -20-3	2.256	99.3	22.71
		Self triggered Tube Tube -20-4	2.414	99.1	24.35
				Average	24.81

Table 2. Quasi- static axial compression test of self triggered tubes at different strain rate

Deformation Rate (mm/min)	**Strain Rate (/s)**	**Specimen Code**	**Energy absorbed(kJ)**	**Mass (gms)**	**Specific Energy Absorbed (kJ/ kg)**
10	1.11x10^{-3}	Self triggered Tube -10-1	2.21	99.3	22.26
		Self triggered Tube -10-2	2.1	99.4	21.13
		Self triggered Tube -10-3	2.2	99.32	22.15
		Self triggered Tube -10-4	2.22	99.4	22.33
				Average	21.97
20	2..22 x10^{-3}	Self triggered Tube -20-1	2.535	99.8	25.40
		Self triggered Tube -20-2	2.666	99.5	26.79
		Self triggered Tube -20-3	2.256	99.3	22.72
		Self triggered Tube -20-4	2.414	99.1	24.36
				Average	24.82
30	3.33 x10^{-3}	Self triggered Tube -30-1	2.75	99.4	27.67
		Self triggered Tube -30-2	2.69	99.3	27.09
		Self triggered Tube -30-3	2.7	99.3	27.19
		Self triggered Tube -30-4	2.71	99.4	27.26
				Average	**27.3**

on the GFRP tubes. Figures 1, 2, 3 and 4 show axial compressive load-displacement graphs of individual GFRP tubes (Non-self-triggered tubes and self-triggered tubes) with inner diameters of 50mm and an outer diameter range from 52 to 52.15 mm also L/d values between 1.91 and 2 all the tubes were compressed at the strain rate of 2.22 x 10^{-3}/s. An assessment of the diagram is shown in Figure 5. the assessment graph reveals that the specific energy absorption value of the composite tubes increases with increasing fiber mat density also the tube fabricated by a mixture all three different density mats recorded the highest specific energy absorption value. Further, the test has concentrated on the self-triggered tube at different strain rate, the test result showed that specific energy absorption value increases with increasing strain rate, prior to dropping somewhat and in this manner settling at around 16.3 kN. Conversely, the graph for the 1.11x10^{-3} strain rate on the GFRP thin-walled tube compressions shows with low compressive force-carrying up to the top at 25 kN, trailed by a lower level worth of roughly 20 kN. In view of the energy absorption under the Load versus displacement curve, the thin-walled GFRP cylinders crushed under 3.33x10^{-3} strain rates offer better energy-absorbing ability. The subsequent energy ingestion esteems for the three cylinders were found to between 13.97 to 24.81 kJ/kg, values that are moderately high for this sort of material. Note that there is not much of a rise in strain rate esteems investigated in this analysis, and the reasoning is very similar to the claims made by Marc Mayer *et al.*[3,5].

9.0 Conclusion

The conclusions that are taken from the studies presented on Non self-triggered GFRP tubes of different density mat and self-triggered tube, crushed under different strain rates with respect to the crushing behavior and evolution of energy absorbing capacity are as follows.

- The tests conducted under controlled low strain rate conditions reveal that, the macro-deformation mechanisms of GFRP tubes at lower strain rates, the failure takes place predominantly by Circumferential cracks, inter-laminar splitting, combined bending and shear modes of deformation.
- For the imposed low strain rates, it is found that, the plateau load increase with the increase in strain rate.
- With an increase in strain rate, the specific energy absorption capacity rises..
- Compared to non-self-triggered tubes, self-triggered tubes have a higher specific energy absorption capacity.

10.0 References

1. Xiao X. Modeling energy absorption with a damage mechanics based composite material model. J Compos Mater. 2009; 43(5):427-4. https://doi.org/10.1177/0021998308097686
2. Bisagni C, Di Pietro G, Fraschini L, Terletti D. Progressive crushing of fiber-reinforced composite structural components of a Formula One racing car. Compos Struct. 2005; 68(4):491-503. https://doi.org/10.1016/j.compstruct.2004.04.015
3. Kim JS, Yoon HJ, Shin KB. A study on crushing behaviors of composite circular tubes with different reinforcing fibers. Int J Impact Eng. 2011; 38(4):198-207. https://doi.org/10.1016/j.ijimpeng.2010.11.007
4. Esmaeili-Marzdashti S, Pirmohammad S, Esmaeili-Marzdashti S. Crashworthiness analysis of s-shaped structures under axial impact loading. Lat Am J Solids Struct. 2017; 14(5):743-64. https://doi.org/10.1590/1679-78253430
5. Reid SR, Reddy TY. Effects of strain rate on the dynamic lateral compression of tubes. Inst Phys Conf Ser No.47, UK: Cambridge; 1979.
6. Chethana KY, Rammohan YS, Patil MG. Prediction of axial load on variable graded composite tubes for crashworthy structure. Mater Today Proc. 2021; 39:1673-6. https://doi.org/10.1016/j.matpr.2020.06.150
7. Mayers M A. Dynamic behavior of materials, John wily and Sons, Inc.; 1994.
8. Chethana KY, Rammohan YS, Patil MG, Reddy LG. Influence of MWCNT addition on mechanical properties of density graded E-glass fiber reinforced polyester resin composites. AIP Conf. Proc. 2019. https://doi.org/10.1063/1.5085611
9. Mayers MA, Chawla KK. Mechanical behavior of materials, Prentice Hall, Inc.; 1998.